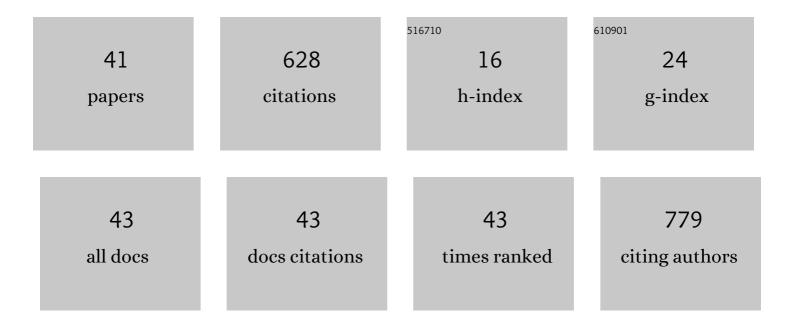
## Andrzej Ostrowski

List of Publications by Year in descending order

Source: https://exaly.com/author-pdf/2895383/publications.pdf Version: 2024-02-01



| #  | Article   | IF  | CITATIONS |
|----|---|-----|-----------|
| 1  | Effects of compositional and structural features on corrosion behavior of nickel–tungsten alloys.<br>Journal of Solid State Electrochemistry, 2009, 13, 263-275.  | 2.5 | 63        |
| 2  | A Simple Route to Alloyed Quaternary Nanocrystals Ag–In–Zn–S with Shape and Size Control.<br>Inorganic Chemistry, 2014, 53, 5002-5012.  | 4.0 | 52        |
| 3  | Cu–Fe–S Nanocrystals Exhibiting Tunable Localized Surface Plasmon Resonance in the Visible to NIR<br>Spectral Ranges. Inorganic Chemistry, 2016, 55, 6660-6669.   | 4.0 | 39        |
| 4  | Ligand exchange in quaternary alloyed nanocrystals – a spectroscopic study. Physical Chemistry<br>Chemical Physics, 2014, 16, 23082-23088.  | 2.8 | 38        |
| 5  | On the Sensitivity of the Ni-rich Layered Cathode Materials for Li-ion Batteries to the Different<br>Calcination Conditions. Nanomaterials, 2020, 10, 2018.   | 4.1 | 33        |
| 6  | Luminophores of tunable colors from ternary Ag–In–S and quaternary Ag–In–Zn–S nanocrystals<br>covering the visible to near-infrared spectral range. Physical Chemistry Chemical Physics, 2017, 19,<br>1217-1228.          | 2.8 | 29        |
| 7  | Highly Luminescent Ag–In–Zn–S Quaternary Nanocrystals: Growth Mechanism and Surface Chemistry<br>Elucidation. Inorganic Chemistry, 2019, 58, 1358-1370.   | 4.0 | 27        |
| 8  | Synthesis and surface chemistry of high quality wurtzite and kesterite Cu2ZnSnS4 nanocrystals using tin(ii) 2-ethylhexanoate as a new tin source. Chemical Communications, 2015, 51, 12985-12988.                         | 4.1 | 24        |
| 9  | Non-injection synthesis of monodisperse Cu–Fe–S nanocrystals and their size dependent properties.<br>Physical Chemistry Chemical Physics, 2016, 18, 15091-15101.  | 2.8 | 23        |
| 10 | Investigation of different ways of activation of fly ash–cement mixtures. Journal of Thermal Analysis<br>and Calorimetry, 2019, 138, 4203-4213.   | 3.6 | 23        |
| 11 | Different strategies of introduction of lithium ions into nickel‑manganese‑cobalt carbonate resulting<br>in LiNi0.6Mn0.2Co0.2O2 (NMC622) cathode material for Li-ion batteries. Solid State Ionics, 2020, 348,<br>115273. | 2.7 | 22        |
| 12 | Suppressing Ni/Li disordering in LiNi0.6Mn0.2Co0.2O2 cathode material for Li-ion batteries by rare earth element doping. Energy Reports, 2022, 8, 3995-4005.  | 5.1 | 22        |
| 13 | Addition of yttrium oxide as an effective way to enhance the cycling stability of LiCoO2 cathode material for Li-ion batteries. Solid State Ionics, 2020, 355, 115426.  | 2.7 | 19        |
| 14 | Organically Modified Aluminophosphates:  Transformation of Boehmite into Nanoparticles and Fibers<br>Containing Aluminodiethylphosphate Tectons. Chemistry of Materials, 2007, 19, 5584-5592.                             | 6.7 | 18        |
| 15 | Microwave Plasma Chemical Vapor Deposition of SbxOy/C negative electrodes and their compatibility<br>with lithium and sodium H¼ckel salts—based, tailored electrolytes. Electrochimica Acta, 2016, 210,<br>395-400.       | 5.2 | 18        |
| 16 | Facile Gram-Scale Synthesis of the First n-Type CuFeS2 Nanocrystals for Thermoelectric Applications.<br>European Journal of Inorganic Chemistry, 2017, 2017, 3150-3153.   | 2.0 | 17        |
| 17 | Kinetic studies of ammonia synthesis over a barium-promoted cobalt catalyst supported on<br>magnesium–lanthanum mixed oxide. Journal of the Taiwan Institute of Chemical Engineers, 2020, 114,<br>241-248.                | 5.3 | 16        |
| 18 | Development of cobalt catalyst supported on MgO–Ln2O3 (Ln = La, Nd, Eu) mixed oxide systems for<br>ammonia synthesis. International Journal of Hydrogen Energy, 2022, 47, 6666-6678.                                      | 7.1 | 16        |

ANDRZEJ OSTROWSKI

| #  | Article   | IF  | CITATIONS |
|----|---|-----|-----------|
| 19 | Synthesis of CuFeS2â~'xSex – alloyed nanocrystals with localized surface plasmon resonance in the visible spectral range. Journal of Materials Chemistry C, 2019, 7, 6246-6250.   | 5.5 | 14        |
| 20 | A high performance barium-promoted cobalt catalyst supported on magnesium–lanthanum mixed oxide for ammonia synthesis. RSC Advances, 2021, 11, 14218-14228.   | 3.6 | 14        |
| 21 | Boosting the Catalytic Performance of Co/Mg/La Catalyst for Ammonia Synthesis by Selecting a<br>Pre-Treatment Method. Catalysts, 2021, 11, 941.   | 3.5 | 13        |
| 22 | Single-crystal and powder X-ray diffraction and solid-state 13C NMR of p-nitrophenyl<br>glycopyranosides, the derivatives of d-galactose, d-glucose, and d-mannose. Carbohydrate Research,<br>2009, 344, 1734-1744.   | 2.3 | 11        |
| 23 | Understanding of Lithium 4,5-Dicyanoimidazolate–Poly(ethylene oxide) System: Influence of the<br>Architecture of the Solid Phase on the Conductivity. Journal of Physical Chemistry C, 2016, 120,<br>23358-23367.   | 3.1 | 8         |
| 24 | From Ag <sub>2</sub> S to luminescent Ag–In–S nanocrystals <i>via</i> an ultrasonic method – an<br><i>in situ</i> synthesis study in an NMR tube. Journal of Materials Chemistry C, 2020, 8, 8942-8952.   | 5.5 | 8         |
| 25 | Heterogeneity induced dual luminescence properties of AgInS <sub>2</sub> and<br>AgInS <sub>2</sub> –ZnS alloyed nanocrystals. Inorganic Chemistry Frontiers, 2021, 8, 3450-3462.  | 6.0 | 8         |
| 26 | Indium(II) Chloride as a Precursor in the Synthesis of Ternary (Ag–In–S) and Quaternary (Ag–In–Zn–S)<br>Nanocrystals. Chemistry of Materials, 2022, 34, 809-825.  | 6.7 | 7         |
| 27 | Linear coordination polymers based on aluminum phosphates: synthesis, crystal structure and morphology. Dalton Transactions, 2016, 45, 8008-8020.   | 3.3 | 6         |
| 28 | Caffeine-Cyclodextrin Complexes as Solids: Synthesis, Biological and Physicochemical Characterization. International Journal of Molecular Sciences, 2021, 22, 4191.   | 4.1 | 6         |
| 29 | Solvent effect in the synthesis of Cu–In–S and Cu–In–Se nanocrystals with tunable structure and composition. Materials Chemistry and Physics, 2015, 162, 291-298.   | 4.0 | 5         |
| 30 | Thermally induced structural transformations of linear coordination polymers based on aluminum tris(diorganophosphates). Dalton Transactions, 2018, 47, 16480-16491.  | 3.3 | 5         |
| 31 | Effect of indium precursor and ligand type on the structure, morphology and surface<br>functionalization of InP nanocrystals prepared by gas–liquid approach. Synthetic Metals, 2014, 187,<br>94-101.   | 3.9 | 4         |
| 32 | Synthesis and crystal growth of microcrystals of the cubic and new orthorhombic polymorphs of (NH4)2SnCl6. Crystal Research and Technology, 2015, 50, 764-768.  | 1.3 | 4         |
| 33 | Systematic Studies on Liquid Sodium 4,5â€dicyanoâ€2â€(trifluoromethyl)imidazolate (NaTDI)â€Based<br>Electrolytes and Its Impact on the Cycling Behaviour Against Wet Impregnated Wlâ€NaNMC and Prussian<br>White Cathodes. Advanced Materials Interfaces, 2022, 9, .                      | 3.7 | 4         |
| 34 | Solid-state structure of methyl<br>2,4,6-tri-O-acetyl-3-O-(2,3,4,6-tetra-O-acetyl-β-d-glucopyranosyl)-β-d-galactopyranoside and methyl<br>3,4,6-tri-O-acetyl-2-O-(2,3,4,6-tetra-O-acetyl-β-d-glucopyranosyl)-β-d-galactopyranoside. Journal of<br>Molecular Structure, 2013, 1037, 49-56. | 3.6 | 3         |
| 35 | 1D and 2D hybrid polymers based on zinc phenylphosphates: synthesis, characterization and applications in electroactive materials. RSC Advances, 2021, 11, 7873-7885.   | 3.6 | 3         |
| 36 | Solid-state structure of N-o-, N-m-, and N-p-nitrophenyl-2,3,4-tri-O-acetyl-β-d-xylopyranosylamines.<br>Carbohydrate Research, 2011, 346, 2491-2498.  | 2.3 | 2         |

| #  | Article   | IF  | CITATIONS |
|----|---|-----|-----------|
| 37 | Single-crystal and powder X-ray diffraction, 13C CP/MAS NMR, and DFT-GIAO calculations of methyl 3,4,6-tri-O-acetyl-2-O-(2,3,4,6-tetra-O-acetyl-Î <sup>2</sup> -d-galactopyranosyl)-α-d-glucopyranoside and methyl 2,4,6-tri-O-acetyl-3-O-(2,3,4,6-tetra-O-acetyl-Î <sup>2</sup> -d-galactopyranosyl)-α-d-glucopyranoside. Journal of Molecular Structure, 2013, 1036, 407-413. | 3.6 | 2         |
| 38 | Crystal and molecular structure of nitrophenyl 2,3,4-tri-O-acetyl-Î <sup>2</sup> -d-xylopyranosides. Journal of<br>Molecular Structure, 2012, 1007, 227-234.  | 3.6 | 1         |
| 39 | Influence of substituents in aryl groups on the structure, thermal transitions and<br>electrorheological properties of zinc bis(diarylphosphate) hybrid polymers. Dalton Transactions,<br>2022, , .   | 3.3 | 1         |
| 40 | GaN growth by sublimation sandwich method. Physica Status Solidi C: Current Topics in Solid State<br>Physics, 2005, 2, 1065-1068.   | 0.8 | 0         |
| 41 | Influence of the Support Composition on the Activity of Cobalt Catalysts Supported on<br>Hydrotalcite-Derived Mg-Al Mixed Oxides in Ammonia Synthesis. Chemistry, 2022, 4, 480-493.   | 2.2 | 0         |